University of New Hampshire
University of New Hampshire Scholars' Repository

Physics Scholarship

Physics

6-2014

Synthesis of 3-D coronal-solar wind energetic particle acceleration modules

Nathan A. Schwadron
University of New Hampshire, Nathan.Schwadron@unh.edu

Matthew J. Gorby
University of New Hampshire, Matthew.Gorby@unh.edu

Tibor Torak
Predictive Science Inc

Cooper Downs
Predictive Science Inc

J. A. Linker
Predictive Science Inc.

See next page for additional authors

Follow this and additional works at: https://scholars.unh.edu/physics_facpub
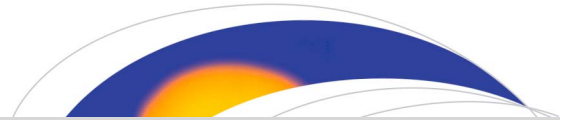
Part of the Physics Commons

Authors
Nathan A. Schwadron, Matthew J. Gorby, Tibor Torak, Cooper Downs, J. A. Linker, Roberto Lionello, Z. Mikic, P. Riley, Joe Giacalone, Benjamin D.G. Chandran, Kai K. Germaschewski, Philip A. Isenberg, Martin A. Lee, Noe E. Lugaz, Sonya S. Smith, Harlan E. Spence, M. Desai, J. C. Kasper, K. Kozarev, K. E. Korreck, M. L. Stevens, J. F. Cooper, and Peter MacNeice

Space Weather

Synthesis of 3-D Coronal-Solar Wind Energetic Particle Acceleration Modules

Nathan A. Schwadron, Matt Gorby, Tibor Török, Cooper Downs, Jon Linker, Roberto Lionello, Zoran Mikić, Pete Riley, Joe Giacalone, Ben Chandran, Kai Germaschewski, Phil A. Isenberg, Martin A. Lee, Noe Lugaz, Sonya Smith, Harlan E. Spence, Mihir Desai, Justin Kasper, Kamen Kozarev, Kelly Korreck, Mike Stevens, John Cooper, and Peter MacNeice

1. Introduction

Acute space radiation hazards pose one of the most serious risks to future human and robotic exploration. Large solar energetic particle (SEP) events are dangerous to astronauts and equipment. The ability to predict when and where large SEPs will occur is necessary in order to mitigate their hazards.

The Coronal-Solar Wind Energetic Particle Acceleration (C-SWEPA) modeling effort in the NASA/NSF Space Weather Modeling Collaborative [*Schunk*, 2014] combines two successful Living With a Star (LWS) (http://lws.gsfc.nasa.gov/) strategic capabilities: the Earth-Moon-Mars Radiation Environment Modules (EMMREM) [*Schwadron et al.*, 2010] that describe energetic particles and their effects, with the Next Generation Model for the Corona and Solar Wind developed by the Predictive Science, Inc. (PSI) group. The goal of the C-SWEPA effort is to develop a coupled model that describes the conditions of the corona, solar wind, coronal mass ejections (CMEs) and associated shocks, particle acceleration, and propagation via physics-based modules.

Assessing the threat of SEPs is a difficult problem. The largest SEPs typically arise in conjunction with X class flares and very fast ($>$1000 km/s) CMEs. These events are usually associated with complex sunspot groups (also known as active regions) that harbor strong, stressed magnetic fields. Highly energetic protons generated in these events travel near the speed of light and can arrive at Earth minutes after the eruptive event. The generation of these particles is, in turn, believed to be primarily associated with the shock wave formed very low in the corona by the passage of the CME (injection of particles from the flare site may also play a role). Whether these particles actually reach Earth (or any other point) depends on their transport in the interplanetary magnetic field and their magnetic connection to the shock.

2. C-SWEPA Models

C-SWEPA combines two main modules:

1. CORHEL, for Corona-Heliosphere, is a coupled set of models and tools for quantitatively modeling the ambient solar corona and solar wind for specific time periods [*Lionello et al.*, 2009; *Riley and Lionello*, 2011; *Riley et al.*, 2012] using photospheric magnetic maps (built up from the Solar Dynamics Observatory Helioseismic and Magnetic Imager, http://hmi.stanford.edu, magnetograms) as boundary conditions. Versions have been released to the multiagency Community Coordinated Modeling Center (CCMC, http://ccmc.gsfc.nasa.gov) located at NASA's Goddard Space Flight Center and to the Air Force Research Laboratory (AFRL) at Kirkland Air Force Base. C-SWEPA uses CORHEL to model CME eruptions in realistic coronal magnetic fields with candidate CME initiation mechanisms. C-SWEPA links CORHEL with EMMREM to explore the implications of CMEs for particle acceleration at shocks low in the corona and deduce the effects for the space radiation environment.

2. EMMREM, for Earth-Moon-Mars Radiation Environment Module, is a tool to describe time-dependent radiation exposure at Earth, Moon, Mars, and interplanetary space environments [*Schwadron et al.*, 2010]. Versions of EMMREM are running at NASA's Space Radiation Analysis Group (SRAG, http://srag-nt.jsc.nasa.gov) and the CCMC, and produce near-real-time data (http://prediccs.sr.unh.edu) at the University of New Hampshire (UNH). A component of EMMREM is the Energetic Particle Radiation Environment Module (EPREM) and is designed to couple with MHD models [*Kozarev et al.*, 2010, 2013] and compute energetic particle distributions along a 3-D Lagrangian grid of nodes that propagate out with the solar wind. Connected lists of node lines form magnetic field lines, which enables highly efficient computation
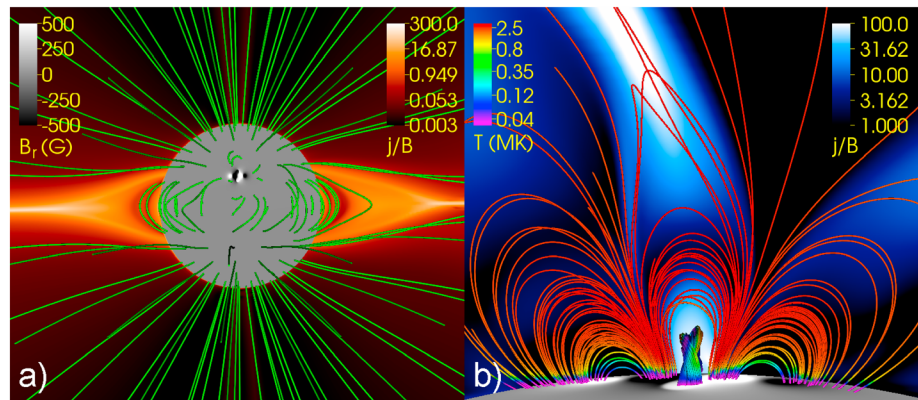
Figure 1. Magnetic field configuration after flux rope insertion and subsequent relaxation. The photospheric radial field, B_r ($r = R_s$), is shown in grayscale. The vertical planes show j/B (in normalized units). (a) The global view of the corona with field lines in green illustrates the field configuration prior to eruption. The j/B color coding illuminates the position of the streamer belt and the heliospheric current sheet. The model active region is located in the Northern Hemisphere. We also focus on the (b) active region where field lines are colored by temperature. The cold (and dense) flux rope core is visible in the center. In this case, the j/B color coding highlights the flux rope and the presence of an additional streamer overlying the active region.

of energetic particle distribution functions at each node. EPREM has been used to solve for pickup ion distributions [*Hill et al.*, 2009; *McComas et al.*, 2008, 2010] and energetic particle distributions [e.g., *Schwadron et al.*, 2010; *Dayeh et al.*, 2010] based on the focused transport equation. The code has been used to span large spatial domains from 0.1 AU to 15 AU and energies from keV up to relativistic GeV energies, which are important for the assessment of radiation hazards and dose-rates [e.g., *Cucinotta et al.*, 2010; *PourArsalan et al.*, 2010]. C-SWEPA extends EPREM for the modeling of shocks, and particle acceleration.

3. Extreme SEP Event Model

We provide here an example of diffusive shock acceleration from a fast CME from the low corona. The CME simulation employed for our analysis will be described in detail in a forthcoming publication (Torok et al., in preparation). Here we restrict ourselves to a brief summary of its main properties.

The simulation is performed using the MAS (Magnetohydrodynamics Around a Sphere) code [e.g., *Mikić and Linker*, 1994; *Mikić et al.*, 1999; *Lionello et al.*, 1999]. The code uses spherical coordinates and advances the standard viscous and resistive MHD equations. It incorporates radiative losses, thermal conduction parallel to the magnetic field, and an empirical coronal heating function. The latter properties are essential for a realistic modeling of the plasma densities and temperatures in the corona and provide the possibility to produce synthetic EUV and soft X-ray images that can directly be compared to observations [see *Lionello et al.*, 2009]. The boundary conditions are discussed by *Linker and Mikić* [1997] and *Linker et al.* [1999].

We consider an idealized solar coronal magnetic configuration, consisting of a global dipole with a field strength of 2 G at the poles and a quadrupolar solar active region (AR) located at ~25°N of the equator. After an MHD solution including a solar wind is obtained by relaxing the system to a steady state [see *Lionello et al.*, 2009], a modified version of the flux rope model by *Titov and Démoulin* [1999], hereafter TDM] is inserted above the central polarity inversion line (PIL) of the AR. Including the flux rope, the model AR has a total magnetic flux of ~7.5×10^{22} Mx and a maximum radial field strength of ~1070 G at the photospheric level. After a fast and strongly dynamic initial adjustment to the surrounding magnetic field, the flux rope evolves toward a numerical equilibrium (Titov et al., submitted). After the relaxation, the free magnetic energy of the AR is about 10^{33} ergs, which is sufficient to power a strong eruption.

Figure 1 gives an impression of the global magnetic field configuration (panel a) and of the active region after the flux rope insertion (panel b) and subsequent relaxation. The global configuration corresponds to solar minimum conditions, with a relatively symmetric heliospheric current sheet that wraps about the equator. Cold (and dense) plasma accumulates in the flux rope during the relaxation, resembling the conditions observed in prominences.
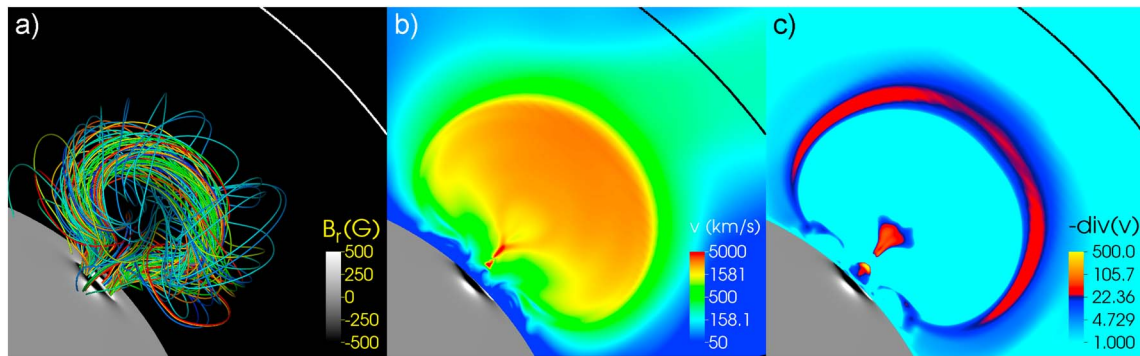
Figure 2. Eruption of the CME: (a) the magnetic field lines of the flux rope superimposed on the radial magnetic field in grayscale at the solar surface; (b) the outward speed of the plasma; and (c) the negative divergence of the plasma velocity, which highlights regions of strong compression. These snapshots of the CME are taken a few minutes after the onset of the eruption. The curved line in the top right corners of each panel indicates the height of two solar radii.

The CME is initiated by triggering the eruption of the TDM flux rope (Figure 1a) [e.g., *Amari et al.*, 2003; *Bisi et al.*, 2010]. Aided by the strong (flare) reconnection jets that occur below the erupting rope, the resulting CME rapidly accelerates to a velocity of ~3000 km s^{-1} low in the corona ($r < 2\,R_s$; Figure 2b), after which it slows down and finally travels with an almost constant speed of ~1000 km s^{-1} at heights $r > 3\,R_s$. This simulation is coupled to a newly developed heliospheric MHD code, and the eruption is propagated to 1 AU [*Lionello et al.*, 2013]. We found that the CME arrives at 1 AU with a speed of ~700 km s^{-1}, still moving significantly faster than the surrounding slow solar wind.

Figure 2 shows the CME eruption: Figure 2a shows the flux rope low in the corona as the CME erupts, Figure 2b shows the outward speed of the plasma within the CME, and Figure 2c shows the divergence of the plasma velocity. The CME-driven shock forms at a height of ~1.4 solar radii. The compression (negative divergence in velocity) is stronger at the flanks of the CME than at its front [*Ontiveros and Vourlidas*, 2009; *Hudson*, 2011]. Figure 2c also shows strong compression in the wake of the CME, as a consequence of reconnection outflows [e.g., *Shibata and Magara*, 2011].

The EPREM model is solved to describe the effects of diffusive shock acceleration and particle acceleration from plasma compression for energetic particles from low in the corona. The model is run out beyond 1 AU across a 3-D domain spanning the inner heliosphere. Output is extracted from an observer at the L1 point location. Generally, we find the most intense and rapid particle acceleration from the regions of strongest compression at the flanks of the CME, as shown in Figure 2c. The case considered is the type of SEP event that is both prompt and very difficult to predict. A key question is whether events of this type could lead to extremely large radiation doses.

The model includes the effects of particle acceleration, adiabatic focusing, parallel and perpendicular diffusive propagation, and drift. We have employed a parallel scattering mean free path that scales as $\lambda_{\parallel} = \lambda_0\,(r/r_1)^{0.15}\,(R_g/R_{g0})^{1/3}$ where r is heliocentric radius, and R_g is particle rigidity. The reference radial distance is $r_1 = 1$ AU, reference rigidity is $R_{g0} = 1$ GV, and reference mean free path is $\lambda_0 = 1$ AU. This leads to characteristic scattering mean free paths of $\lambda_{\parallel} \sim 0.1$–0.5 AU from 1 to 100 MeV at 1 AU. We have also adopted a fixed ratio of perpendicular-to-parallel diffusion, $\kappa_{\perp}/\kappa_{\parallel} \approx 0.01$ [e.g., *Giacalone and Jokipii*, 1999].

We used quiet time ^{4}He ion (0.10.5 MeV/nuc) observations from ACE/ULEIS for the suprathermal preevent spectrum [*Dayeh et al.*, 2009]. We converted the spectrum to protons assuming the flux is scaled via an inverse square dependence, and a He/H ratio of 10%. Differential energy fluxes in Figure 3 (top right) show that rapid particle acceleration leads to relatively high particle fluxes for energies up to ~1 GeV at 1 AU. The abrupt rise-time is associated with shock acceleration low in the corona during the rapid lateral expansion of the CME. By coupling the state-of-the-art MHD model (CORHEL) with EMMREM, C-SWEPA takes the next logical step needed by the Space Weather community to predict doses associated with intense SEP radiation.

The massive parallelization of the EPREM model has allowed us to incorporate thousands of magnetic field lines in the uniquely adaptive 3-D EPREM grid. Cross-field diffusion and drift are accurately specified through communication across neighboring magnetic field lines in the EPREM grid [*Schwadron et al.*, 2010; *Kozarev et al.*, 2010]. Cross-field diffusion is critical in contributing to broad longitudinal distributions, particularly
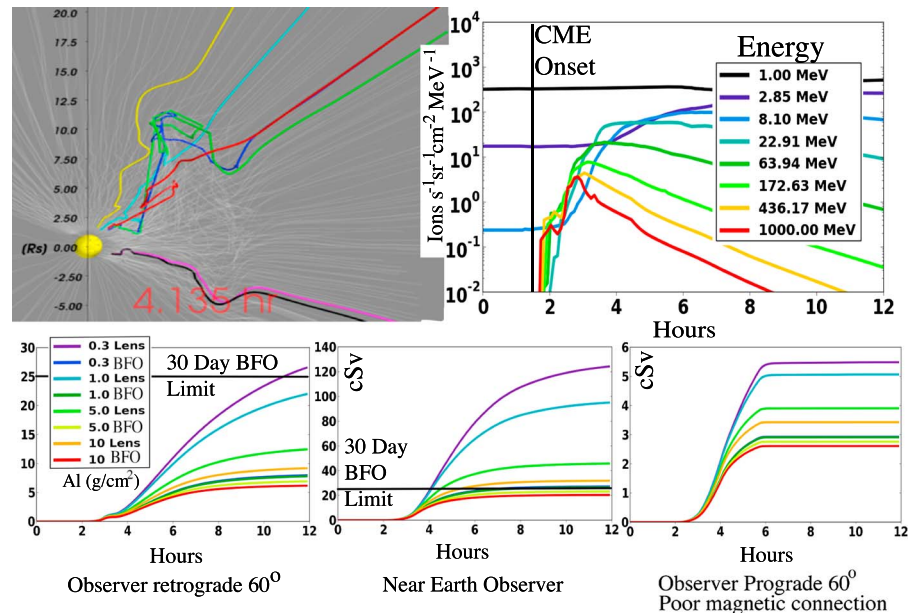
Figure 3. Energetic particles are accelerated over a broad latitudinal and longitudinal spread from the CME released following destabilization shown in Figure 2. (left top) The colored magnetic field lines show strong distortions by the plasma flow. Using coupled MAS-EPREM simulations, we link coronal conditions, CMEs and associated shocks, and transients to (top right) solar energetic particles, solar wind conditions (Figure 1), and (bottom) time-dependent radiation exposure. Shown in the right top panel and bottom panels are the results for particle differential energy fluxes at 1 AU from the event shown in Figure 2. Figure 3 (bottom) shows the resulting integrated dose equivalents for Lens and Blood Forming Organs (BFO) behind different levels of shielding. The results here show tens of cSv even for well-shielded (10 g/cm^2 Al) BFO dose equivalents, indicating a radiation hazard that approaches the 30 day limit (25 cSv) in roughly 2 h after CME initiation. In the simulation time history, the CME onset begins at l= 1.43 h, and then strong compression and energetic particle acceleration begins at 1.45 h. Integrated doses at prograde (Figure 3, bottom right) and retrograde observers (Figure 3, bottom left) are shown in addition to the near-Earth observer. Note that the retrograde observer is better connected magnetically to the CME driver, which explains the higher and more prolonged SEP fluxes at this observer.

during the evolution of particle acceleration and propagation while shock drivers propagate from low in the corona. Figure 3 illustrates the importance of the process. Prograde and Retrograde observers are placed ±60° with respect to the L1 (near Earth) observer (Figure 3). Even a low level of perpendicular diffusion (1% of the parallel diffusion coefficient) provides sufficient cross-field transport to affect these widely separated observers.

4. Conclusions

Described here is the development of a new project, the Coronal-Solar Wind Energetic Particle Acceleration (C-SWEPA) Modules, which couples the CORHEL MHD models within the low corona with EMMREM for characterizing energetic particle acceleration and subsequent formation of energetic particle hazards. We have shown initial results of the coupling, in which an extreme SEP event with a broad longitudinal extent was formed from a fast CME at 2–5 solar radii. This model showed large enough differential energy fluxes to approach 30 day radiation limits even behind thick spacecraft shielding (10 g/cm^2). The fact that the event was so abrupt, with high-energy fluxes formed within only 2 h after CME onset, demonstrates the significant potential hazard for astronauts and spacecraft. The development of accurate predictive models, response strategies, and an understanding of the statistical probability for this type of prompt and extreme SEP event is the focus of C-SWEPA research in the NASA/NSF Space Weather Modeling Collaborative [Schunk, 2014].

References

Amari, T., J. F. Luciani, J. J. Aly, Z. Mikic, and J. Linker (2003), Coronal mass ejection: Initiation, magnetic helicity, and flux ropes. I. Boundary motion-driven evolution, *Astrophys. J.*, *585*, 1073–1086, doi:10.1086/345501.
Bisi, M. M., et al. (2010), From the Sun to the Earth: The 13 May 2005 coronal mass ejection, *Sol. Phys.*, *265*, 49–127, doi:10.1007/s11207-010-9602-8.
Cucinotta, F. A., et al. (2010), Space radiation risk limits and Earth-Moon-Mars Environmental Models, *Space Weather*, *8*, S00E09, doi:10.1029/2010SW000572.

Dayeh, M. A., et al. (2009), Composition and spectral properties of the 1 AU quiet-time suprathermal ion population during solar cycle 23, *Astrophys. J.*, *693*, 1588, doi:10.1088/0004-637X/693/2/1588.

Dayeh, M. A., et al. (2010), Modeling proton intensity gradients and radiation dose equivalents in the inner heliosphere using EMMREM: May 2003 solar events, *Space Weather*, *8*, S00E07, doi:10.1029/2009SW000566.

Giacalone, J., and J. R. Jokipii (1999), The transport of cosmic rays across a turbulent magnetic field, *Astrophys. J.*, *520*, 204–214, doi:10.1086/307452.

Hill, M. E., N. A. Schwadron, D. C. Hamilton, R. D. Difabio, and R. K. Squier (2009), Interplanetary suprathermal He+ and He++ observations during quiet periods from 1.5 to 9 AU and implications for particle acceleration, *Astrophys. J. Lett.*, *699*, L26–L30, doi:10.1088/0004-637X/699/1/L26.

Hudson, H. S. (2011), Global properties of solar flares, *SSR*, *158*, 5–41, doi:10.1007/s11214-010-9721-4.

Kozarev, K. A., R. M. Evans, N. A. Schwadron, M. A. Dayeh, M. Opher, K. E. Korreck, and B. van der Holst (2013), Global numerical modeling of energetic proton acceleration in a coronal mass ejection traveling through the solar corona, *Astrophys. J.*, *778*, 43, doi:10.1088/0004-637X/778/1/43.

Kozarev, K., et al. (2010), Modeling the 2003 Halloween Events with EMMREM: Energetic particles, radial gradients, and coupling to MHD, *Space Weather*, *8*, S00E08, doi:10.1029/2009SW000550.

Linker, J. A., and Z. Mikić (1997), Extending coronal models to Earth orbit, in *Coronal Mass Ejections*, AGU, Washington, D. C.

Linker, J. A., Z. Mikić, D. A. Biesecker, R. J. Forsyth, S. E. Gibson, A. J. Lazarus, A. Lecinski, P. Riley, A. Szabo, and B. J. Thompson (1999), Magnetohydrodynamic modeling of the solar corona during whole Sun month, *J. Geophys. Res.*, *104*, 9809–9830, doi:10.1029/1998JA900159.

Lionello, R., Z. Mikić, and J. A. Linker (1999), Stability of algorithms for waves with large flows, *J. of Comp. Phys.*, *152*, 346–358.

Lionello, R., J. A. Linker, and Z. Mikic (2009), Multi-spectral emission of the Sun during the first whole Sun month: MHD simulations, *Astrophys. J.*, *690*, 902–912, doi:10.1088/0004-637X/690/1/902.

Lionello, R., C. Downs, J. A. Linker, T. Török, P. Riley, and Z. Mikić (2013), Magnetohydrodynamic simulations of interplanetary coronal mass ejections, *Astrophys. J.*, *777*, 76, doi:10.1088/0004-637X/777/1/76.

McComas, D. J., et al. (2008), The solar wind around Pluto (SWAP) aboard new horizons, *Space Sci. Rev.*, *140*, 261–313, doi:10.1007/s11214-007-9205-3.

McComas, D. J., H. A. Elliott, and N. A. Schwadron (2010), Pickup hydrogen distributions in the solar wind at ~ 11 AU: Do we understand pickup ions in the outer heliosphere?, *J. Geophys. Res.*, *115*, A03102, doi:10.1029/2009JA014604.

Mikić, Z., and J. A. Linker (1994), Disruption of coronal magnetic field arcades, *Astrophys. J.*, *430*, 898–912.

Mikić, Z., J. A. Linker, D. D. Schnack, R. Lionello, and A. Tarditi (1999), Magnetohydrodynamic modeling of the global solar corona, *Phys. Plasmas*, *6*, 2217, doi:10.1063/1.873474.

Ontiveros, V., and A. Vourlidas (2009), Quantitative measurements of coronal mass ejection-driven shocks from LASCO observations, *Astrophys. J.*, *693*, 267–275, doi:10.1088/0004-637X/693/1/267.

PourArsalan, M., et al. (2010), Time-dependent estimates of organ dose and dose equivalent rates for human crews in deep space from the 26 October 2003 solar energetic particle event (Halloween event) using the Earth-Moon-Mars Radiation Environment Module, *Space Weather*, *8*, S00E05, doi:10.1029/2009SW000533.

Riley, P., and R. Lionello (2011), Mapping solar wind streams from the Sun to 1 AU: A comparison of techniques, *Solar Physics*, *270*, 575–592, doi:10.1007/s11207-011-9766-x.

Riley, P., J. A. Linker, R. Lionello, and Z. Mikic (2012), Corotating interaction regions during the recent solar minimum: The power and limitations of global MHD modeling, *J. Atmos. Sol. Terr. Phys.*, *83*, 1–10.

Schunk, R. W. (2014), NASA/NSF Space Weather Modeling Collaboration: Advancing Space Weather Modeling for improved specification, forecasting, and mitigation, *Space Weather*, *12*, 131, doi:10.1002/2014SW001049.

Schwadron, N. A., et al. (2010), Earth-Moon-Mars Radiation Environment Module framework, *Space Weather*, *8*, S00E02, doi:10.1029/2009SW000523.

Shibata, K., and T. Magara (2011), Solar flares: Magnetohydrodynamic processes, *Living Rev. Sol. Phys.*, *8*, 6.

Titov, V. S., and P. Démoulin (1999), Basic topology of twisted magnetic configurations in solar flares, *Astron. Astrophys.*, *351*, 707–720.

Nathan A. Schwadron is an Associate Professor of Physics and a member of the Institute for Study of Earth, Oceans and Space at the University of New Hampshire.

Matthew Gorby is in Information Technologist working at Space Science Center at the University of New Hampshire.

Tibor Török is a Research Scientist at Predictive Science Inc., San Diego, CA.

Cooper Downs is a Research Scientist at Predictive Science Inc., San Diego, CA.

Jon Linker is President of Predictive Science Inc.

Roberto Lionello is a Research Scientist ad Predictive Science Inc. in San Diego, California.

Zoran Mikicacute is a Senior Research Scientist at Predictive Science, Inc., in San Diego, California.

Pete Riley a Senior Scientist at Predictive Science Inc.

Joe Giacalone is a Professor of Planetary Sciences at the University of Arizona.

Benjamin D. G. Chandran is a Professor of Physics and member of the Institute for the Study of Earth, Oceans, and Space at the University of New Hampshire.

Kai Germaschewski is an Assistant Professor of Physics and a member of the Institute for Study of Earth, Oceans and Space at the University of New Hampshire.

Philip A. Isenberg is a Research Professor of Physics and a member of the Institute for the Study of Earth, Oceans and Space at the University of New Hampshire.

Martin A. Lee is a Professor of Physics and a member of the Institute for Study of Earth, Oceans and Space at the University of New Hampshire.

Noé Lugaz is a Research Assistant Professor of Physics and a member of the Institute for Study of Earth, Oceans and Space at the University of New Hampshire.

Sonya Smith is a Project Manager and a member of the Institute for Study of Earth, Oceans and Space at the University of New Hampshire.

Harlan E. Spence is Director of the Institute for the Study of Earth, Oceans and Space and a Professor of Physics at the University of New Hampshire.

Mihir Desai is a Staff Scientist at the Southwest Research Institute in San Antonio, Texas.

Justin C. Kasper is an Associate Professor in the Atmospheric, Oceanic, and Space Sciences Department at the University of Michigan.

Kamen A. Kozarev is a NASA LWS Jack Eddy Postdoctoral Fellow at the Smithsonian Astrophysical Observatory.

Kelly Korreck is an astrophysicist at the Smithsonian Astrophysical Observatory.

Michael L. Stevens is an astrophysicist at the Smithsonian Astrophysical Observatory.

John F. Cooper is Chief Scientist of the NASA Space Physics Data Facility and a senior research scientist with the Heliospheric Physics Laboratory of the Heliophysics Science Division at NASA Goddard Space Flight Center.

Peter MacNeice is a Research Astrophysicist in the Heliophysics Science Division at NASA, Goddard Space Flight Center.